INL/CON-21-64910-Revision-0

Accelerated Coupled Monte Carlo-Thermal Hydraulic Calculations using a Hybrid GTF-Diffusion-based Prediction Block: First Results

May 2022

Bailey Painter, Dan Kotlyar, Stefano Terlizzi

Changing the World's Energy Future

Idaho National Laboratory

INL is a U.S. Department of Energy National Laboratory operated by Battelle Energy Alliance, LLC

INL/CON-21-64910-Revision-0

Accelerated Coupled Monte Carlo-Thermal Hydraulic Calculations using a Hybrid GTF-Diffusion-based Prediction Block: First Results

Bailey Painter, Dan Kotlyar, Stefano Terlizzi

May 2022

Idaho National Laboratory
Idaho Falls, Idaho 83415

http://www.inl.gov

Prepared for the
U.S. Department of Energy
Under DOE Idaho Operations Office
Contract DE-AC07-05ID14517

Accelerated Coupled Monte Carlo-Thermal Hydraulic Calculations using a Hybrid GTF-Diffusion-based Prediction Block: First Results

Bailey Painter[1], Stefano Terlizzi[2], and Dan Kotlyar[1*]

[1]Georgia Institute of Technology
North Avenue NW, Atlanta, GA 30332

[2]Idaho National Laboratory
1955 N Fremont Ave, Idaho Falls, ID 83415

painter@gatech.edu, stefano.terlizzi@inl.gov, dan.kotlyar@me.gatech.edu

ABSTRACT

Accurate predictions of spatial power and temperature distributions require the coupling of a neutron transport solver with a thermal-hydraulic (TH) feedback. Nowadays, Monte Carlo (MC) codes are widely coupled to TH solvers, typically via a Picard iteration (PI) method, due to the higher fidelity that such frameworks can produce. To speed up a PI, a prediction step can produce an improved initial guess for a source distribution and feed it to the MC code. Recent work [1, 2] investigated a prediction step that uses generalized transfer functions (GTFs) to predict the macroscopic cross sections' variations following a perturbation in TH properties, such as coolant density. The previous method also relied on first order perturbation (FOP) theory to predict perturbed power profiles, rather than using an expensive MC iterate. The implemented FOP method relied on generating a fission matrix from which the forward and adjoint eigenmodes were extracted and later used to for power calculations. The generation of the fission matrix can introduce a significant computational overhead, therefore undermining the performance of the proposed hybrid technique when applied to high-dimensional problems, *e.g.,* full core calculations. This work attempts to improve the GTF-FOP prediction step by replacing the FOP solver with a nodal diffusion solver, thus eliminating the need to calculate a fission matrix. The GTF-diffusion step was tested for various moderator density perturbations. In each case, the predicted power distribution showed good agreement with the reference case. The latter is attributed to the generally good prediction of most spatially distributed macroscopic cross sections, except the transport cross section, which will become the focus of future work.

KEYWORDS: Multiphysics, Monte Carlo, Thermal Hydraulics, Transfer Functions, Cross sections

1. INTRODUCTION

Among the numerical techniques used to couple Monte Carlo (MC) neutronic codes and Thermal Hydraulic (TH) codes, the Picard iteration (PI) scheme is the most used in steady state calculations. Its simple implementation allows single-physics codes to be leveraged without carrying out changes in the source code level. However, the convergence rate of the PI is only linear in absence of statistical uncertainties. To

speed up the convergence rate of the PI scheme, several approaches have been proposed. Among these is the use of an acceleration block relying on a lower order neutronic model [1, 2]. In Ref. [2], the acceleration was obtained by concatenating two sub-blocks. The first one used the Generalized Transfer Function (GTF) theory to update the mono-energetic macroscopic cross sections after a change in temperature and density conditions [3, 4]. The second sub-block used first order perturbation (FOP) theory to estimate the corresponding value of the power distribution and the associated effective multiplication factor. In the FOP sub-block, the fission matrix from the last MC solution is used to estimate the eigenvalues and the corresponding eigenvectors of the one-group neutron flux.

The combined GTF-FOP block method has two main benefits over conventional methods for cross sections prediction. First, GTFs can be computed on-the-fly, without altering the source code of the TH and MC codes. Second, it can account for the spatial effects of perturbations as the cross sections and transfer functions are produced from 3-dimensional calculations. The main drawback to the GTF-FOP method is that it requires the eigenvectors and eigenmodes of the flux. These eigenvalues and eigenvectors are approximated using the eigenvectors of the fission source, computed from the fission matrix. However, the fission matrix is computationally expensive to obtain, as its cost is squared with the number of meshes in a problem. A single fission matrix can be used to predict perturbations for multiple iterations, but its cost for larger scale problems can increase calculation time in one Picard step by 10-folds.

To improve the shortcomings of the original GTF-FOP acceleration this paper presents preliminary results on the use of a nodal diffusion (ND) solver for the power prediction in lieu of first order perturbation theory. The integrated scheme will be denoted here as the GTF-ND prediction block, and it retains all the advantages of the GTF-FOP block, while eliminating the computational cost associated to the fission matrix calculation. This block will accelerate the calculation of problems characterized by higher dimensionality, *i.e.,* full-core problems. The remainder of this paper is structured as follows. Section 2 discusses the general methodology of the GTF-ND prediction block, including the theory of the GTF sub block. Section 3 reports the numerical results obtained with the new GTF-ND acceleration block for an extruded BWR unit-cell. Finally, Section 4 presents the conclusions and discusses future work.

2. METHODOLOGY AND IMPLEMENTATION

Section 2.1 reports a summary of the GTF theory for the sake of a self-contained paper. The discussion will be limited to changes in moderator density, here denoted by $\boldsymbol{\rho}$**.** For the complete theory, please refer to [2]. Section 2.2 presents details on the acceleration block implementation.

2.1. Summary of the GTF theory

The GTF is a linear operator mapping the input variable ρ to the corresponding system response Σ, where input and outputs are projected in suitable vector bases. Choosing the Fourier discrete basis for the output variable space and the Krylov basis for the input variable space leads to the following expressions for the GTF associated to the macroscopic cross section Σ_x:

$$\widetilde{H}_x = \frac{\sum_{n=0}^{N} \rho^{(n)} \tilde{\Sigma}_{n.x}}{\tilde{\rho}}. \tag{1}$$

- $\rho^{(n)}$ denotes the projection of the variable ρ on the nth Krylov basis vector, ψ_n, such that:

$$\rho = \sum_{n=0}^{N} \rho^{(n)} \psi_n \tag{2}$$

- $\tilde{\Sigma}_{n.x}$ is the discrete Fourier transform of the macroscopic cross section spatial profile Σ_x, associated to an input variable with spatial profile ψ_n.
- $\tilde{\rho}$ is the discrete Fourier transform of the input variable ρ.

If $|\rho^{(0)}| \gg |\rho^{(n)}|$, and the expansion coefficients are normalized such that $\rho^{(0)} = 1$, then the single-shape approximation of the GTF is obtained:

$$\widetilde{H}_x = \frac{\tilde{\Sigma}_{0.x}}{\tilde{\rho}}. \tag{3}$$

Eq. 3 describes the frequency-domain response of the system to the input variable ρ.

2.2. Implementation of the GTF-ND Prediction Block

The Picard Iteration (PI) is the simplest coupling strategy for MC and TH codes in steady-state conditions. In this algorithm, a MC simulation is run to obtain the expected power profile. The power is then fed into the TH code, and density and temperature profiles are computed. These profiles are then used in the MC code, and the sequence is repeated until convergence is achieved. This algorithmic sequence is represented in Fig. 1.a. The convergence rate of the standard PI scheme is at most linear, assuming negligible MC-related uncertainties. However, the convergence rate can be increased by inserting a prediction block between the TH and the MC block as shown in Fig. 1.b. The function of this prediction block is to produce a better estimation of the fission source spatial distribution with respect to the ones computed at the previous iteration, therefore leading to a faster convergence. In Refs. 1 and 2, this prediction block was composed of three sub-blocks: (1) A TH sub-block to compute updated temperature and density profiles, (2) a GTF sub-block to predict the cross sections associated to the new TH conditions, and (3) a power prediction sub-block based on first order perturbation theory. In this work, the power prediction is performed with a nodal diffusion (ND) solver, rather than a first order perturbation theory. The definition and implementation of this prediction block is the focus of this paper. Future work will focus on fully coupling the prediction block with a Picard iteration scheme.

The steps for the GTF-ND prediction block are depicted in Fig.1.c and are detailed below:

1. *Initial conditions*: The cross sections spatial distributions $\Sigma_0(x)$ and the power spatial distribution are obtained from the MC at the previous iteration. For simplicity, this paper will only focus on the effect of perturbations in the moderator densities $\rho(x)$.

2. *GTF Calculation*: The TFs $\widetilde{H}$ are calculated for each initial macroscopic cross section $\Sigma_0(x)$ using the initial TH data $\rho_0(x)$ as an input. In this paper, the TFs for the one-group macroscopic absorption cross section, fission cross section, and transport cross section are computed, using Eq. 3. For instance, in the case of the transport cross section:

$$\widetilde{H}_{\Sigma_{tr}} = \frac{\tilde{\Sigma}_{tr}}{\tilde{\rho}_0}, \tag{4}$$

   Where $\tilde{\Sigma}_{tr}$ is the DFT of the macroscopic transport cross section and $\tilde{\rho}_0$ is the DFT of the initial density. The TFs were calculated using the python package transientGTF, a python-based code developed at the Georgia Institute of Technology for cross section storage and manipulation. The tool interfaces with serpentTools to read and automatically store cross section data from SERPENT output files [5, 6]. The transientGTF is currently hosted on a private repository, however, the authors are planning to make it public in the near future.

3. *TH prediction*. The sub-channel TH code THERMO is used to compute the density profile ρ_1 and the temperature profile T_1 with the power profile inputted at step 1 [7].

4. *Inverse Transform*. The one-group macroscopic cross sections are predicted using the transfer functions computed at step 2:

$$\Sigma_{tr,1} = \mathcal{F}^{-1}\left(\tilde{H}_{\Sigma_{tr}}\,\tilde{\rho}_1\right). \tag{5}$$

$\mathcal{F}^{-1}$ is the inverse DFT, $\tilde{\rho}_1$ is the DFT of the perturbed density profile, and $\Sigma_{tr,1}$ is the predicted perturbed macroscopic transport cross section spatial distribution.
The inverse transform in this paper was performed using the transientGTF code.

6. *ND Solver*: The predicted, perturbed cross sections are fed into a ND solver to obtain a predicted, perturbed source distribution. In this work, the DYN3D diffusion code is used to compute the updated power profile [8].

7. *Results*: The predicted, perturbed power spatial distribution and effective multiplication factor is fed into the MC solver as an improved initial guess for the next iteration.

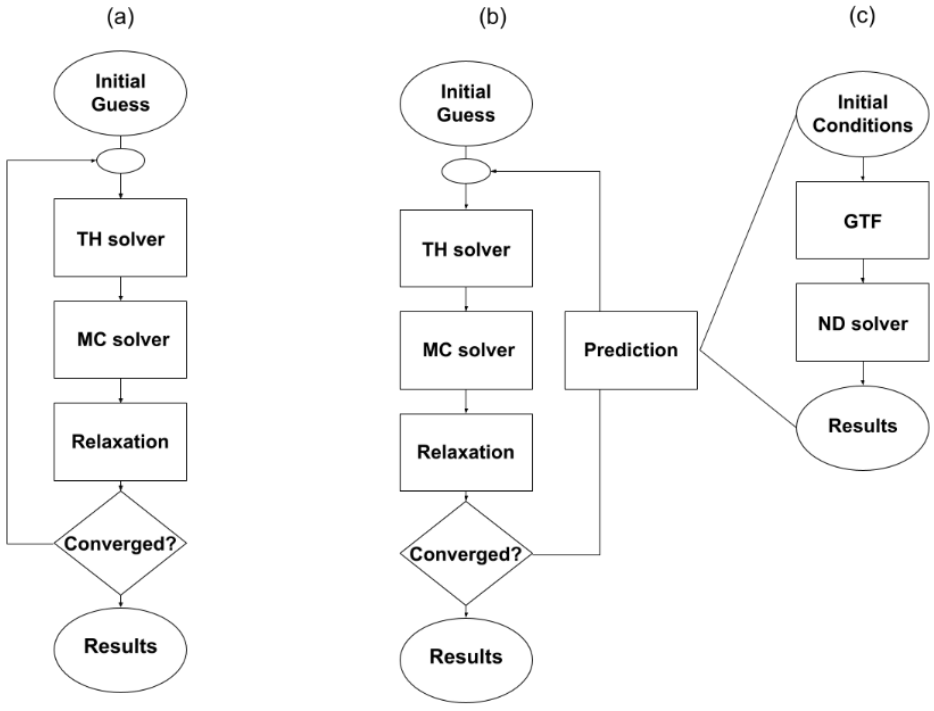

Figure 1. (a) Flow diagrams for a standard PI with an MC solver, (b) an alternate PI with an MC solver and prediction block, and (c) the GTF-ND prediction block.

3. RESULTS

3.1. Test Problem description

The test case investigated in this paper is an extruded BWR unit-cell, *i.e.,* fuel pin surrounded by water, with axial reflectors. Geometric values are shown in Table I. The moderator density distribution was varied for different input files as shown in Fig. 2.a-c, while the fuel temperature was held constant. The focus of this section is to demonstrate how different levels of perturbation in the moderator density affect the GTF-ND accuracy.

Table I. BWR Unit-Cell Problem Specifications

Parameter	Value
Total height (cm)	405.760
Top axial reflector height (cm)	20
Bottom axial reflector height (cm)	20
Pellet radius (cm)	0.60579
Gas-gap radius (cm)	0.62103
Cladding radius (cm)	0.71501
Pitch (cm)	1.87452
Gas-gap density (g/cm^3)	1.0004×10^{-3}
Zr cladding density (g/cm^3)	6.5514
UO2 density (g/cm^3)	10.42

3.2. Perturbation of Macroscopic Cross Sections in the GTF block

The ability of the ND block to produce an accurate prediction of the perturbed fission source spatial profile depends on the ability of the GTF block to produce an accurate prediction of the perturbed, one-group macroscopic cross sections. In this paper, three different test cases relating to the perturbation of the coolant density are investigated: a far perturbation, a middle perturbation, and a close perturbation. The mean absolute percent error (MAPE) between the initial density and the perturbed density for each of these cases is 22.8%, 5.97%, and 2.49% respectively. The results of the predicted cross sections are shown in Fig. 2. For conciseness, the macroscopic fission cross section has been omitted from the plots since it follows the same trends as the absorption cross section, *i.e.*, both depend more on fuel properties than the moderator properties. The predicted fission cross section is still used to obtain the results in section 3.3.

From Fig. 2, it is evident that the GTF block does a good job at predicting the perturbed shape of the cross sections, but overpredicts the change in magnitude. The error is greatest in the transport cross section which depends on both the total scattering cross section and the average scattering cosine angle of neutrons ($\bar{\mu}_0$) as shown in Eq. 6. In these test cases, $\bar{\mu}_0$ should change after the perturbation because the average moderator number density decreases while the average fuel number density stays the same. According to Eq. 7, this increased contribution of the fuel would result in a lower scattering angle – and consequently, a higher transport cross section – due to the heavier nuclei in the fuel [9]. As a result, the real, perturbed transport cross section has a greater magnitude than the predicted perturbed result in each case.

$$\Sigma_{tr} = \Sigma_t - \bar{\mu}_0 \Sigma_s \tag{6}$$

$$\bar{\mu}_0 \approx \frac{2}{3}\frac{\sum_j \frac{\Sigma_{s,j}}{A_j}}{\sum_j \Sigma_{s,j}} \tag{7}$$

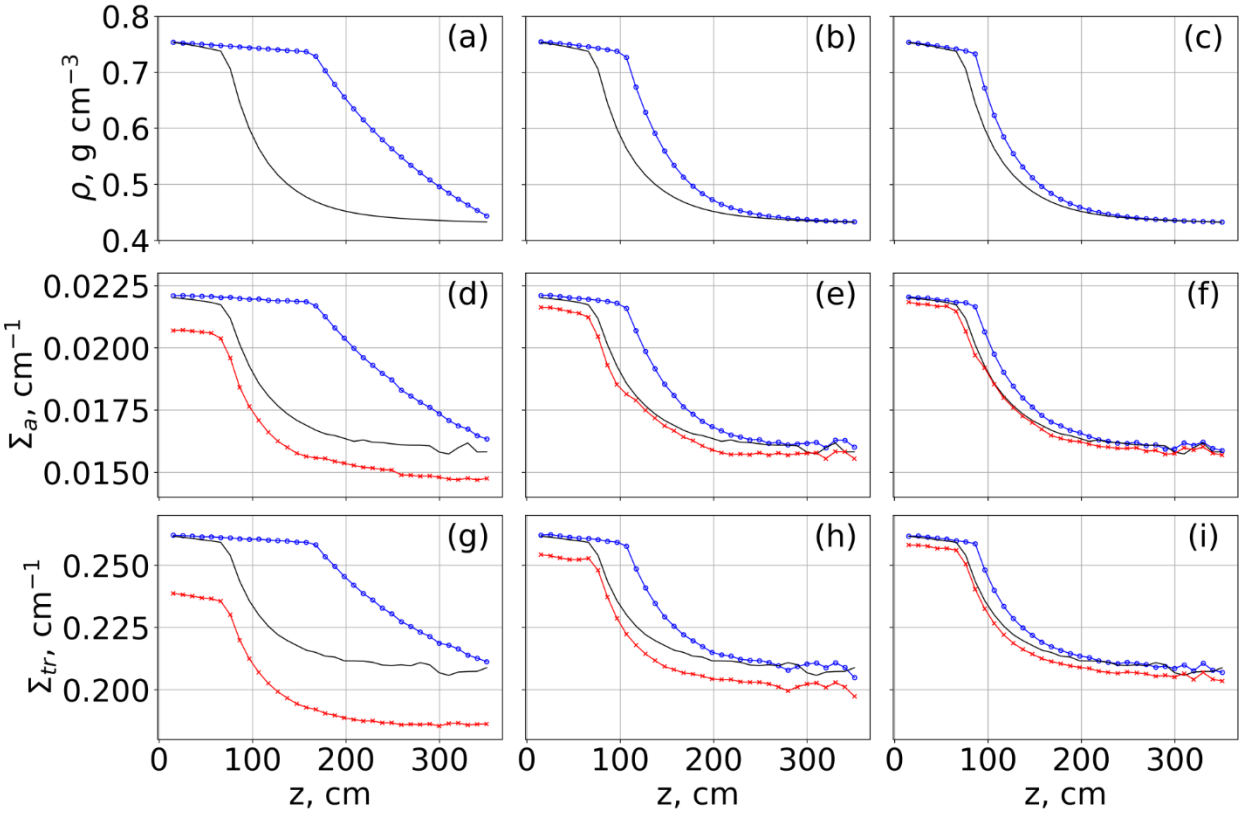

Figure 2. From left to right, results for a far perturbation (a, d, h), a middle perturbation (b, e, h), and a close perturbation (c, f, i). From top to bottom, moderator densities (a, b, c), macroscopic absorption cross sections (d, e, f), and macroscopic transport cross sections (g, h, i). The blue line represents an initial state, the red line represents a predicted final state, and the black line represents the reference final state.

3.3. Power perturbations

To demonstrate the accuracy of the ND solver independently from the GTF performance, a known set of density-perturbed cross sections were obtained directly from Serpent and fed into DYN3D. This case is denoted here as 'DYN3D direct'. Figs. 3-5 present the power profiles obtained directly with Serpent for the reference and perturbed densities. Although, the macroscopic cross sections are fed as mono-energetic, DYN3D obtains nearly the same results as SERPENT as reaction rates are properly preserved.

The prediction block that uses DYN3D as the ND solver performs has non-negligible discrepancy in the power distribution. This is expected due to the poorer prediction of the transport cross section using the GTF approach. Future work will investigate improving the prediction of the transport cross section. Still, the results do show that DYN3D functions well as a one-group prediction tool.

Figs. 3-5 compare the output of the GTF-ND block to the reference solution and the 'DYN3D direct' solution. Table II summarizes the MAPE between the initial and final state as well as the MAPE between the predicted and final solution in regions that contribute to greater than 1% of the total power. Regions with less than 1% power were excluded from this metric as they are more sensitive to noise and will inherently have higher errors. It is noticeable that the GTF-ND block performs well in all cases, including the "far-perturbation" case. In this latter case, the GTF-ND block predicts power with a MAPE of only 4.33% where the initial guess had an MAPE of 40.3%. Table II also gives a figure of merit (FOM) value for the prediction as the ratio of the MAPE of the initial guess to the MAPE of the prediction. This FOM decreases as the initial guess approaches the reference solution. Predictions based on improved initial guesses will therefore slowly approach the MAPE of the direct solution, 0.691%.

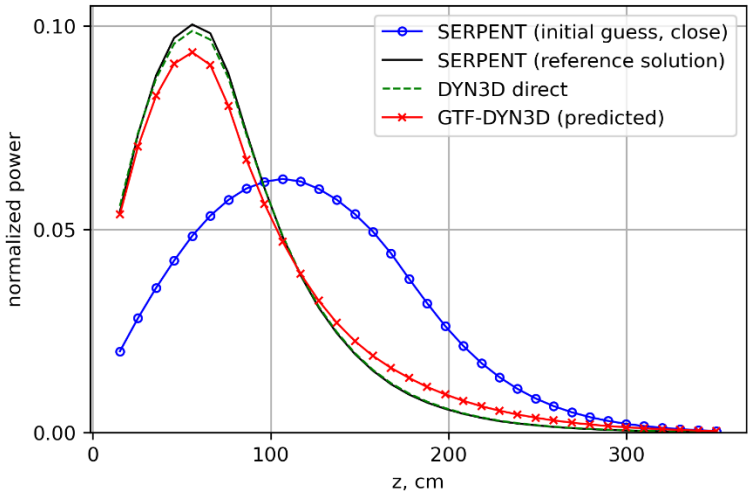

Figure 3. Normalized power profile results when perturbing from a far initial guess

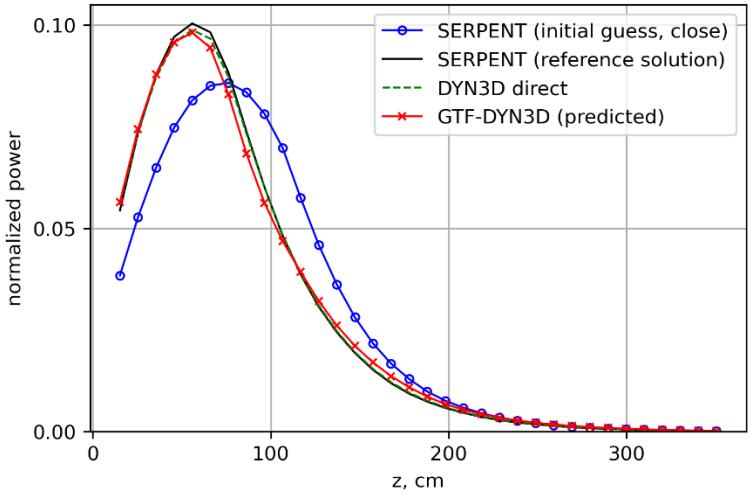

Figure 4. Normalized power profile results when perturbing from a middle initial guess

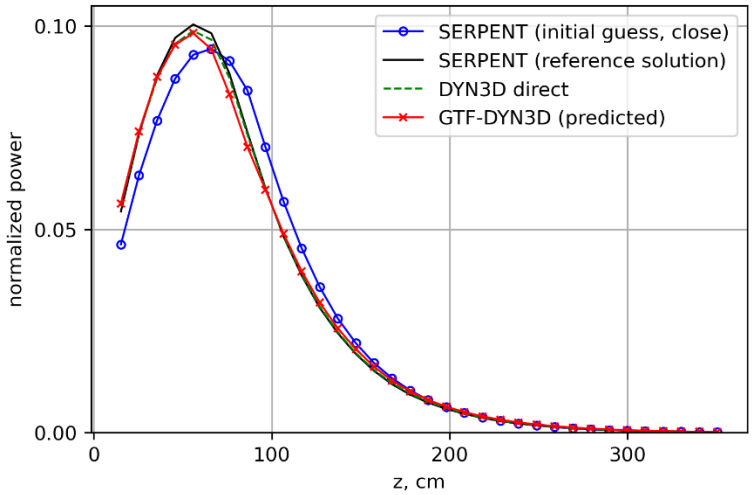

Figure 5. Normalized power profile results when perturbing from a close initial guess

Table II. MAPE between initial and final states and between predicted and final states

perturbation	MAPE - initial	MAPE - prediction	FOM
far	40.3%	4.33%	9.31
middle	14.9%	2.55%	5.84
close	6.07%	1.83%	3.31

4. CONCLUSION

This work has demonstrated the potential of the GTF-ND sub-block to replace the GTF-FOP sub-block proposed in Refs. [2, 4]. The GTF sub-block was able to predict with good accuracy the spatial shape variation in the fission, absorption, and transport macroscopic cross sections after a density perturbation. The maximum error was found for the transport cross section, mainly due to the inability to capture the dependence of the transport cross section on the scattering angle and the fuel-moderator ratio in the cell. Despite the error in the transport cross sections prediction in correspondence of large perturbations, the ND solver was still able to estimate the power profile within a MAPE of 5% in every case.

The GTF prediction method relies on linear operators theory to compute the transfer functions for the macroscopic cross sections. This means that the GTF approach is valid only for "small" perturbations of the initial density. The maximum magnitude of the perturbation to obtain an accurate cross section prediction has not been determined for a general problem. However, based on the authors' experience, both the GTF-ND and GTF-FOP sequences can perform a prediction within few percent of the target power profile if the density varies within. 40% in L_2 norm between the initial profile and the target density profile. [2]. Future works will thoroughly investigate and discuss this limitation of the GTF approach.

Future work will also be devoted to enhancing the accuracy of the transport macroscopic cross section's prediction and to coupling the GTF-ND block with a TH-MC PI. The latter task will allow for assessment of the GTF-ND block's potential to reduce the number of MC and TH iterations, similar to the results shown in Refs. [2-4].

ACKNOWLEDGEMENTS

The authors would like to thank Framatome Inc. for their funds and support in developing stochastic-deterministic modeling and simulation capabilities.

REFERENCES

1. B. R. Herman, B. Forget, and K. Smith, "Progress toward Monte Carlo–thermal hydraulic coupling using low-order nonlinear diffusion acceleration methods," *Annals of Nuclear Energy*, **84**, pp. 63-72, (2015).
2. S. Terlizzi and D. Kotlyar, "On-the-fly prediction of macroscopic cross-section spatial response to th perturbations through transfer functions: Theory and first results," *Nuclear Science and Engineering*, **194**(4), pp. 280-296 (2020).
3. S. Terlizzi and D. Kotlyar, "A perturbation-based acceleration for Monte Carlo – Thermal Hydraulics Picard iterations. Part I: Theory and application to extruded BWR unit-cell," *Annals of Nuclear Energy*, **167**, (2022).
4. S. Terlizzi and D. Kotlyar, "A perturbation-based acceleration for Monte Carlo – Thermal Hydraulics Picard iterations. Part II: Application to 3D PWR-based problems," *Annals of Nuclear Energy*, **166**, (2022).
5. J. Leppänen et al., "The Serpent Monte Carlo Code: Status, Development and Applications in 2013," *Annals of Nuclear Energy*, **82**, pp. 142 (2015).
6. A.E. Johnson, D. Kotlyar, S. Terlizzi, and G. Ridley, "serpentTools: A python package for expediting analysis with serpent," *Nuclear Science and Engineering*, **194**, pp. 1016 (2020).
7. E. E. Y. Shaposhnik and E. Shwageraus, "Thermal-Hydraulic Feedback Module for BGCore System," *Proceedings of the 25th Conference of Nuclear Societies in Israel*, Dead Sea, Israel, (2010).
8. U. Rohde, V.A. Pivovarov, and Y.A. Matveev, "Studies on boiling water reactor design with reduced moderation and analysis of reactivity accidents using the code DYN3D-MG," *Kerntechnik*, **77**, pp. 240–248, (2012).
9. J.J. Duderstadt and L.J. Hamilton, *Nuclear Reactor Analysis*, pp. 110-130, John Wiley & Sons, Hoboken, NJ, USA (1975).